Reconfigurable origami-inspired acoustic waveguides

Sahab Babaee, Johannes T B Overvelde, Elizabeth R Chen, Vincent Tournat, Katia Bertoldi

APPLIED SCIENCES AND ENGINEERING

Reconfigurable origami-inspired acoustic waveguides

Sahab Babaee,[1] Johannes T. B. Overvelde,[1,2] Elizabeth R. Chen,[1] Vincent Tournat,[1,3] Katia Bertoldi[1,4]*

We combine numerical simulations and experiments to design a new class of reconfigurable waveguides based on three-dimensional origami-inspired metamaterials. Our strategy builds on the fact that the rigid plates and hinges forming these structures define networks of tubes that can be easily reconfigured. As such, they provide an ideal platform to actively control and redirect the propagation of sound. We design reconfigurable systems that, depending on the externally applied deformation, can act as networks of waveguides oriented along one, two, or three preferential directions. Moreover, we demonstrate that the capability of the structure to guide and radiate acoustic energy along predefined directions can be easily switched on and off, as the networks of tubes are reversibly formed and disrupted. The proposed designs expand the ability of existing acoustic metamaterials and exploit complex waveguiding to enhance control over propagation and radiation of acoustic energy, opening avenues for the design of a new class of tunable acoustic functional systems.

INTRODUCTION

Acoustic waveguides designed to direct sound are ubiquitous and can be found in cars, buildings, jet engines, medical devices, and musical instruments, to name just a few. Although most of the proposed acoustic waveguides consist of a single duct, it is well known that carefully connected tubes can result in significant transmitted noise reduction (*1*, *2*). Moreover, it has also been shown that the propagation of acoustic waves in tubes arranged to form a square lattice can be successfully described with tools from solid-state physics and provides opportunities to control sound through dispersion and band gaps (*3*). Finally, three-dimensional networks of waveguides have been used to study sound propagation in regular urban areas (*4*). Although these examples illustrate the potential of acoustic waveguides with more complex geometry, they only cover a small region of the available design space, and a natural question to ask is how the geometry of the three-dimensional networks of tubes affects the propagation of sound.

Origami (*5*)—the ancient art of paper folding—not only results in intricate and aesthetically pleasant designs but also provides an ideal platform for the design of transformable mechanical metamaterials. In particular, two-dimensional sheets folded along predefined creases have enabled the design of multistable structures (*6*–*9*), materials with negative Poisson's ratio (*10*–*12*) and tunable stiffness (*13*), and topological metamaterials (*14*). Although most of the proposed origami-like metamaterials are based on two-dimensional folding patterns, snapology (*15*, *16*)—a modular origami technique—has recently inspired the design of highly reconfigurable three-dimensional metamaterials assembled from extruded polyhedra (*17*). These designs also result in interconnected and reconfigurable networks of tubes defined by the assembly of rigid plates and elastic hinges. Here, we combine experiments and simulations to demonstrate that such three-dimensional networks of tubes can be exploited to design reconfigurable acoustic waveguides capable of efficiently controlling and redirecting the propagation of sound.

[1]John A. Paulson School of Engineering and Applied Science, Harvard University, Cambridge, MA 02138, USA. [2]Foundation for Fundamental Research on Matter (FOM) Institute AMOLF, Science Park 104, 1098 XG Amsterdam, Netherlands. [3]LUNAM Université, Université du Maine, CNRS, LAUM UMR 6613, Av. O. Messiaen, 72085 Le Mans, France. [4]Kavli Institute, Harvard University, Cambridge, MA 02138, USA.
*Corresponding author. Email: bertoldi@seas.harvard.edu

RESULTS

Reconfigurable acoustic waveguides based on extruded cubes

We start by considering a three-dimensional mechanical metamaterial consisting of a cubic array of connected extruded cubes (see Fig. 1). If we assume that all the faces are rigid and the structure can only fold along the edges, this periodic structure will have three degrees of freedom identified by the angles α_1, α_2, and α_3 (*17*). Changing these three angles not only deforms the assembly of plates into numerous specific shapes but also significantly alters the network of channels defined by them (see Fig. 1 and movie S1), providing an ideal platform for the design of reconfigurable acoustic waveguides.

More specifically, for $(\alpha_1, \alpha_2, \alpha_3) = (\pi/2, \pi/2, \pi/2)$, the system is fully expanded and comprises a three-dimensional network of interconnected channels oriented in three perpendicular directions (Fig. 1A). In this configuration, the tubes are acoustically coupled, and we expect the radiation by the structure to take place in all three directions, covering the entire surrounding space without a specific directivity. Differently, for $(\alpha_1, \alpha_2, \alpha_3) = (\pi/2, \pi/2, 0)$ and $(\alpha_1, \alpha_2, \alpha_3) = (\pi/3, 2\pi/3, \pi/3)$, the channels are all parallel to each other (Fig. 1, B and C), such that sound waves can only propagate in one direction. However, for $(\alpha_1, \alpha_2, \alpha_3) = (\pi/2, \pi/2, 0)$, the channels are disjointed, whereas for $(\alpha_1, \alpha_2, \alpha_3) = (\pi/3, 2\pi/3, \pi/3)$, they are all connected. Therefore, for $(\alpha_1, \alpha_2, \alpha_3) = (\pi/2, \pi/2, 0)$, we expect the system to behave as a classical single-tube waveguide, whereas for $(\alpha_1, \alpha_2, \alpha_3) = (\pi/3, 2\pi/3, \pi/3)$, we expect the additional wave interferences in the structure to result in a more complex frequency response and a variety of radiation patterns.

To demonstrate our ideas, we numerically and experimentally investigate the propagation of sound waves through the proposed reconfigurable metamaterial. In the simulations, we construct three-dimensional models of the metamaterial comprising a $4 \times 4 \times 4$ cubic array of extruded cubes and deform them into the three different configurations shown in Fig. 1. The plates forming the structure are considered as reflective rigid boundaries, and the air inside and around the resulting tubes is meshed using acoustic elements (Abaqus element type AC3D10M). Moreover, nonreflecting boundary conditions are imposed on the outer boundaries of the acoustic medium to avoid the reflection of energy back into it. Finally, acoustic waves are excited by applying a harmonically varying pressure to one of the openings (highlighted in red in Fig. 1), and the steady-state dynamic linearized response

of the system is calculated for a wide range of frequencies using the commercial finite element package Abaqus 6.12 (Simulia, Providence, RI).

Furthermore, we fabricate a centimeter-scale prototype of the metamaterial from polymeric sheets (PET) and double-sided tape, using a stepwise layering and laser-cutting technique (see Materials and Methods for more details) (*17*, *18*). To measure the transmission response of the three-dimensional waveguide, acoustic waves are excited through air inside the tubes using a loudspeaker placed at one end of one of the tubes (depicted by the red S in Fig. 2). Then, the amplitudes of both the excited and scattered pressure waves are recorded using two microphones (model 378B02, PCB Piezotronics) mounted near the input loudspeaker (point S) and outlets (point A). Finally, the transmittance is computed in decibels as the ratio between the output and input amplitude signals [that is, $20\mathrm{Log}_{10}\|A_A(f)/A_S(f)\|$]. Note that during the tests, the sample is surrounded by sound-absorbing foam to lower the influence of spurious reflections outside the structure and mimic free-field conditions. These foam layers were removed before taking the pictures shown in Fig. 2, for better visualization.

In Fig. 3, we focus on the configuration defined by $(\alpha_1, \alpha_2, \alpha_3) = (\pi/2, \pi/2, 0)$ and present our combined numerical and experimental results for the propagation and radiation of the acoustic waves generated by a source located at one of the openings (highlighted in red in

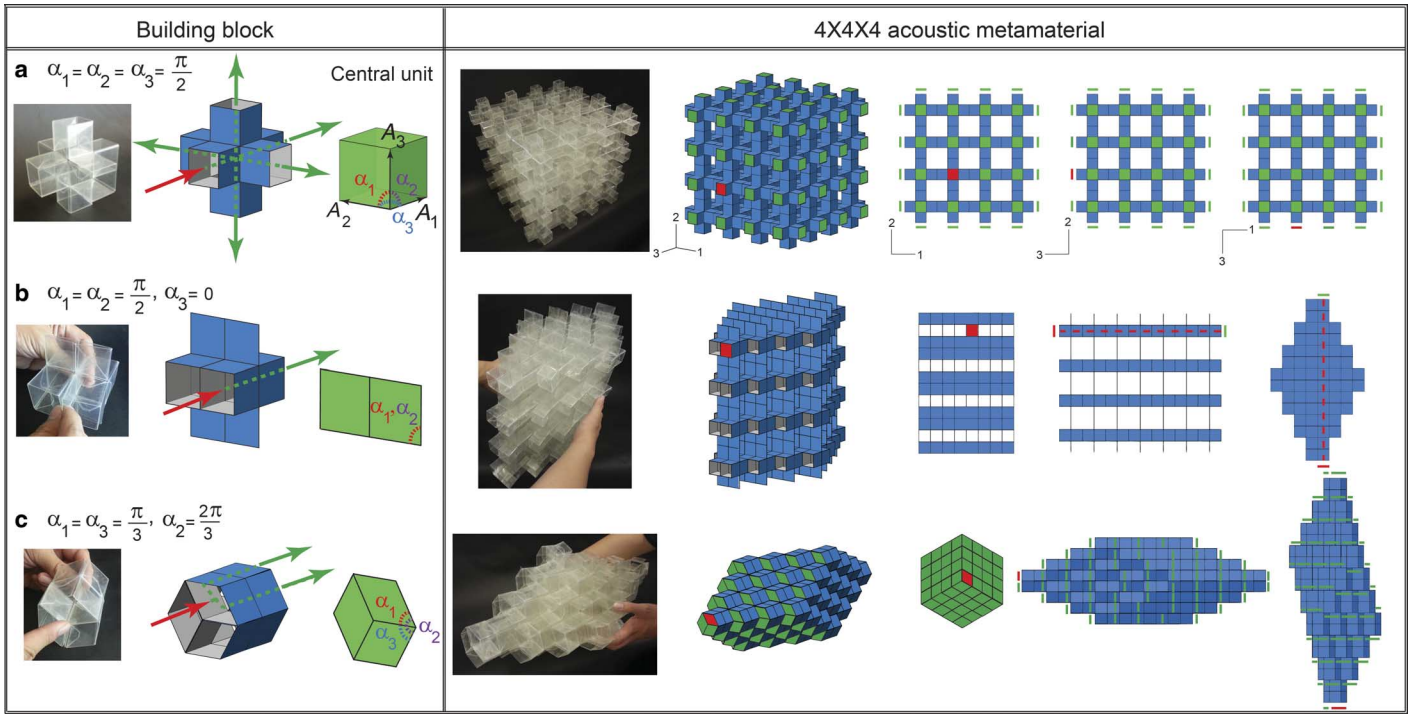

Fig. 1. Reconfigurable origami-inspired acoustic waveguides. Experimental and actual models of the building block (the extruded cube) and the corresponding reconfigurable acoustic metamaterial deformed into three different configurations: (a) $(\alpha_1, \alpha_2, \alpha_3) = (\pi/2, \pi/2, \pi/2)$, (b) $(\alpha_1, \alpha_2, \alpha_3) = (\pi/2, \pi/2, 0)$, and (c) $(\alpha_1, \alpha_2, \alpha_3) = (\pi/3, 2\pi/3, \pi/3)$. The red arrows and shaded areas indicate the excited waves, whereas the green arrows and shaded areas highlight the points from which the structure radiates.

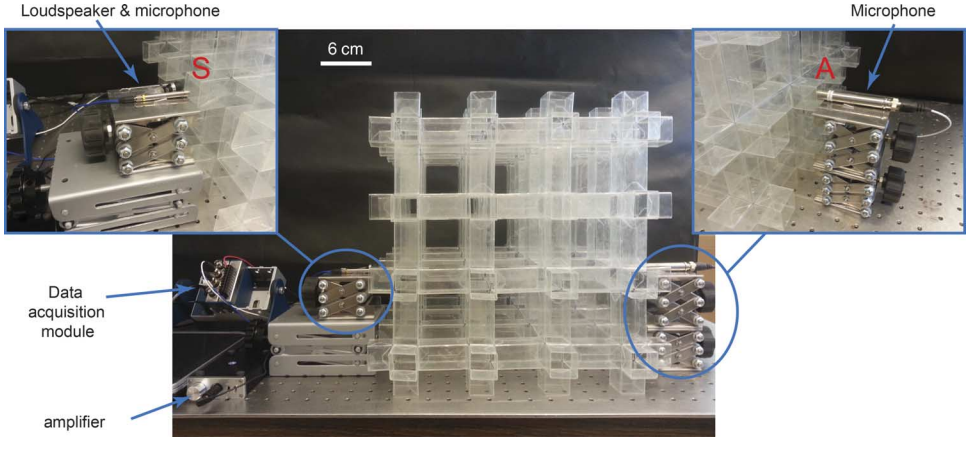

Fig. 2. Experimental setup. Experimental setup without the sound-absorbing foam surrounding the sample.

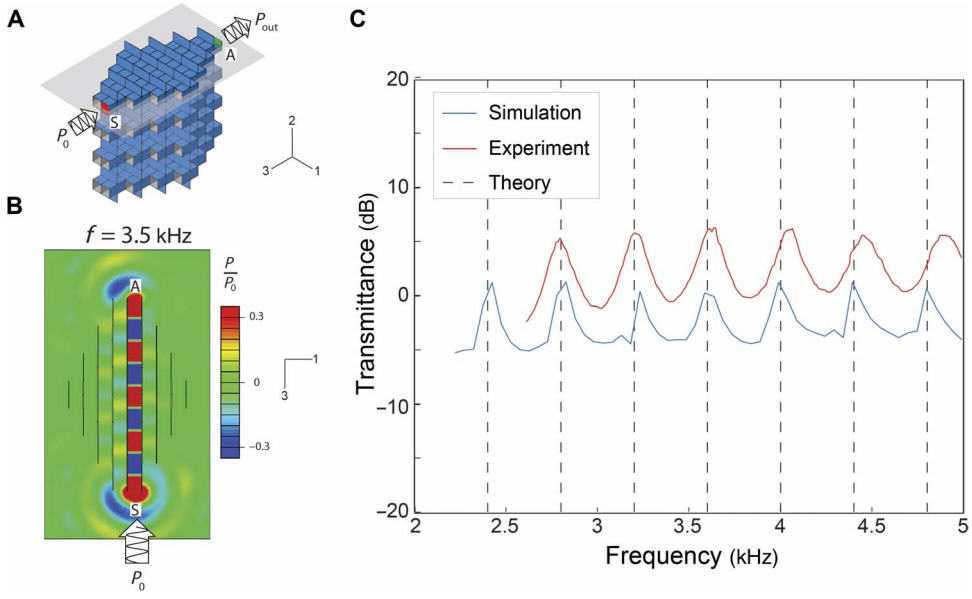

Fig. 3. Propagation of sound waves for (α_1, α_2, α_3) = (π/2, π/2, 0). (**A**) Model of the metamaterial. (**B**) Top cross-sectional view of the pressure field distribution at f = 3.5 kHz. The cutting plane is shown in (A), and the color indicates the pressure amplitude normalized by the input signal amplitude (P_0). (**C**) Frequency-dependent transmittance for the sample where experimental (red lines), numerical (blue line), and analytical (dashed black lines) results are shown.

Fig. 3A). Because the tubes are all parallel and disconnected from each other in this configuration, the system behaves as a single-tube waveguide. As such, the acoustic energy remains mostly confined in the excited tube with weak radiation out of the structure (Fig. 3B and fig. S1), and its frequency response is characterized by regularly spaced resonances (corresponding to the peaks of the transmittance curve reported in Fig. 3C) (*19*). It is well known that such resonance frequencies can be analytically predicted by solving the Helmholtz equation for the pressure field (*20*). In particular, for an individual channel of length L with a square cross section of edge a, rigid side walls, and zero-pressure condition at the two ends, the resonance frequencies are given by

$$f_{lmn} = \frac{c_0}{2\pi}\sqrt{\left(\frac{l\pi}{a}\right)^2 + \left(\frac{m\pi}{a}\right)^2 + \left(\frac{n\pi}{L}\right)^2} \quad (1)$$

where c_0 = 343.2 m/s is the speed of sound in air and l, m, and n are the three integers characterizing the waveguide modes. Because $L = 14a$ in our system, its lowest modes are characterized by $l = m = 0$ and correspond to standing plane waves along the tube. For a = 3 cm (as in our prototype), nonplanar modes across the waveguide section can propagate only for $f > f_{100} = f_{010} = c_0/2a$ = 5.7 kHz. We also note that, although Eq. 1 provides a good qualitative estimation of the resonances of the tube, it is insufficient for quantitative comparison with experiments (*21*). The wave radiation at the open ends of the tube results in a deviation from the zero-pressure condition considered in deriving Eq. 1. Classically, this effect can be accounted for by adding a correction length 2δ to the physical length L of the tube, which depends on the details of the tube geometry. Here, by comparing analytical and numerical results, we find agreement for $\delta = 0.3a$, so that the resonance frequencies of the planar modes are given by $f_{00n} = nc_0/[2(L + 0.6a)]$. Finally, we find agreement between our analytical, numerical, and experimental results (see Fig. 3C), with only a few decibel-level discrepancies between simulated and experimental curves. These discrepancies are mainly due to the inexact placement of the speaker and microphone at the tube opening in the experiments as well as to the small influence of the speaker/microphone presence on the wave field.

Next, in Fig. 4, we present results for the configuration defined by (α_1, α_2, α_3) = (π/3, 2π/3, π/3). Although the channels are all oriented along the same direction in this case, they have a rhombic cross section and are interconnected throughout the structure. Consequently, when deformed into this state, the metamaterial is characterized by a totally different acoustic response. This is demonstrated in Fig. 4 (A and B), where we show the transmittance calculated using two different detection points (denoted as A and B in Fig. 4C). Both curves exhibit strong and complex frequency dependence, originating from the interferences that occur inside the system because the waves can follow a myriad of different paths when traveling from the source to the receiver owing to the multiple interconnections. We also find that the connectivity of the tubes reduces the average level of the transmittance over the studied frequency range to around −20 dB, which is significantly lower than that measured for the configuration of Fig. 3. Moreover, it should be noted that, for this case, quantitative agreement between simulated and experimental transmittances is not reached. This is because the geometric imperfections (submillimeter holes in the corners and narrow gaps between the folded rigid faces, inherent to the origami design; see fig. S2) play a much bigger role than in the case of a single-tube waveguide because they significantly alter the path followed by the traveling waves and, consequently, the wave interferences. Finally, we find that not only the transmittance but also the radiation patterns are strongly frequency-dependent (movie S3). For example, at 2 kHz, the wave radiation by the structure gives rise to frontward quasi-plane waves, whereas at 4.8 kHz, the wave fronts are more curved and show complex spatial patterns (Fig. 4C). We find that at 4.8 kHz, the modes propagating in the tubes are also nonplanar, although f is <5.7 kHz. This is due to the interconnections between air channels that increase the effective width of the waveguide structure.

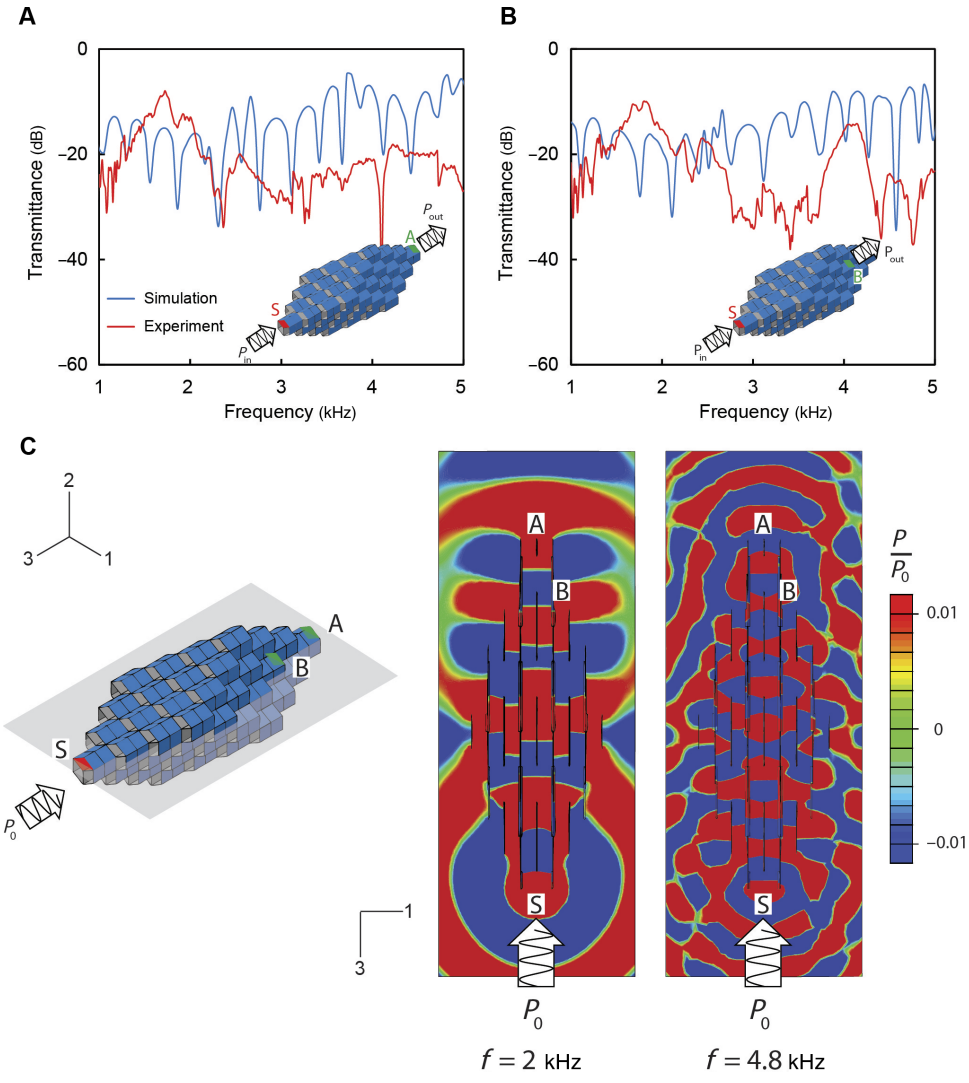

Fig. 4. Propagation of sound waves for (α_1, α_2, α_3) = (π/3, 2π/3, π/3). (**A** and **B**) Frequency-dependent transmittances of the sample calculated considering two different detection points. Both experimental (red lines) and numerical (blue lines) results are shown. (**C**) Model of the metamaterial and top cross-sectional view of the pressure field distribution at f = 2 and 4.8 kHz. The cutting plane is shown in gray (left), and the color map indicates the pressure amplitude normalized by the input signal amplitude P_0 (right).

Consequently, we expect a multimodal propagation in the structure to start at lower frequencies (typically ~2 kHz) than those calculated in the case of the independent single tubes [that is, for (α_1, α_2, α_3) = (π/2, π/2, 0)].

Finally, in Fig. 5, we focus on the expanded state of the system defined by (α_1, α_2, α_3) = (π/2, π/2, 0), where the waveguides are interconnected and oriented in three orthogonal directions. Similar to the case of Fig. 4 (A and B), the transmittance curves reported in Fig. 5 (A and B) have an average value of ~20 dB and show a complex frequency dependence. Because of the waveguide interconnections, numerous interferences from the possible paths come into play even in the case of detection at point A, which is aligned with the source. Moreover, because the waveguides are oriented in three different directions, the wave radiation by the structure covers the entire surrounding space (Fig. 4, C and D, and movie S4), and we observed much smaller radiated amplitude behind the structure (oppositely to the source) than for the previous configurations of aligned waveguides.

Reconfigurable acoustic waveguides based on different extruded polyhedra

Although so far we have focused on a metamaterial comprising a cubic array of extruded cubes, the proposed strategy to design reconfigurable acoustic waveguides is not restricted to this specific geometry. A wealth of three-dimensional reconfigurable networks of tubes capable of qualitatively different deformation can be realized by taking convex polyhedra as templates and extruding arbitrary combinations of their polygonal faces.

As an example, in Fig. 6, we consider a metamaterial based on a periodic array of truncated octahedra. Although the resulting structure is rigid if all the faces of the truncated octahedra are extruded, here, we construct a metamaterial with a single degree of freedom (denoted by θ in Fig. 6A) by extruding the eight green hexagonal faces (highlighted in green in Fig. 6A), removing four of the square faces (highlighted in yellow in Fig. 6A), and making the two remaining ones rigid (highlighted in blue in Fig. 6A). As for the case of the metamaterial based

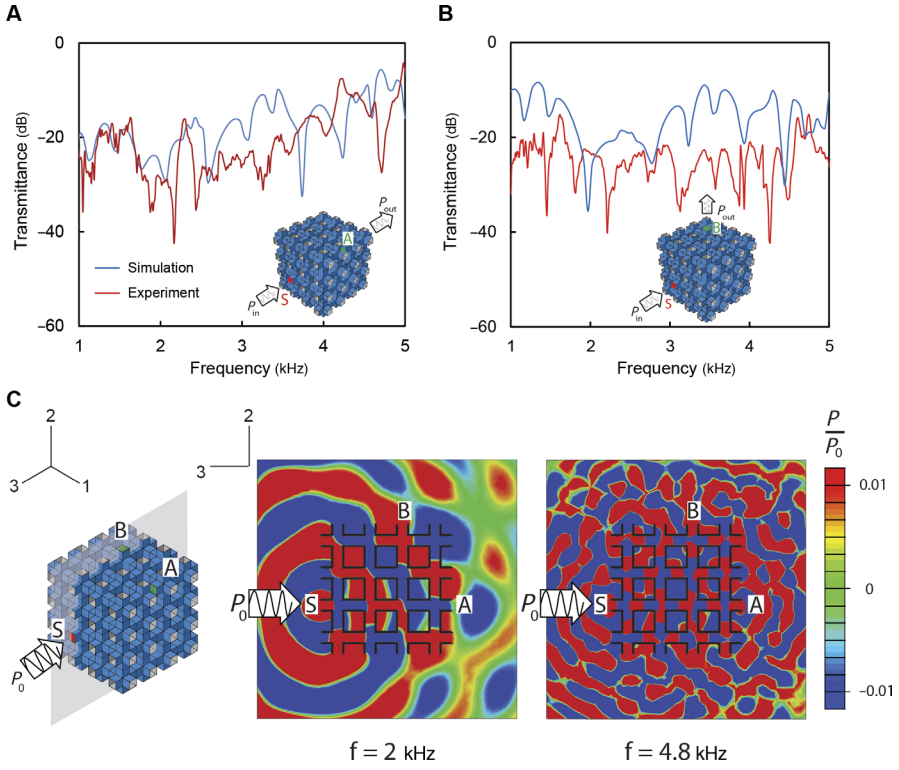

Fig. 5. Propagation of sound waves for $(\alpha_1, \alpha_2, \alpha_3) = (\pi/2, \pi/2, \pi/2)$. (**A** and **B**) Frequency-dependent transmittances of the sample calculated considering two different detection points. Both experimental (red lines) and numerical (blue lines) results are shown. (**C**) Model of the metamaterial and cross-sectional view of the pressure field distribution at $f = 2$ and 4.8 kHz. The cutting plane is shown in gray (left), and the color map indicates the pressure amplitude normalized by the input signal amplitude P_0 (right).

on the extruded cubes, by changing θ between 0 and π/2, the architecture of the system can be transformed (see Fig. 6, fig. S4, and movie S5). However, in the case of $0 < \theta < \pi/2$, the metamaterial does not act as an acoustic waveguide because it does not comprise a network of interconnected tubes (Fig. 6A). Only for $\theta = 0$ and $\theta = \pi/2$ do the plates defining the structures form interconnected channels that can be used to guide acoustic waves. More specifically, for $\theta = 0$, all tubes are parallel and disconnected (Fig. 6B) so that the system behaves as a single-tube waveguide and has an identical response to the extruded cube waveguide for $(\alpha_1, \alpha_2, \alpha_3) = (\pi/2, \pi/2, 0)$ (see Fig. 3). Differently, for $\theta = \pi/2$, the folded structure functions as a two-dimensional waveguide (see the red arrow in Fig. 6C). This example highlights another interesting feature of our metamaterials: the ability to switch the guiding of acoustic energy on and off, because the networks of tubes can be reversibly formed and disrupted for certain configurations.

Finally, we use extruded hexagonal prisms to construct a system that can act as a one-, two-, or three-dimensional waveguide (Fig. 7). More specifically, the building block of this structure is a hexagonal prism with all its faces extruded, except for two square faces that are kept rigid (highlighted in blue in Fig. 7A). The metamaterial formed by connecting these extruded unit cells is highly deformable and characterized by two degrees of freedom, denoted by α and γ in Fig. 7A. Differently from the structures considered in Fig. 6, here, the assembly of plates and hinges forms a network of tubes that can be exploited as an acoustic waveguide for any admissible combination of (α,γ). In the expanded configuration defined by (α,γ) = (0,0), the structure acts as a three-dimensional waveguide because the excited waves (red arrow in Fig. 7A) can propagate along three different

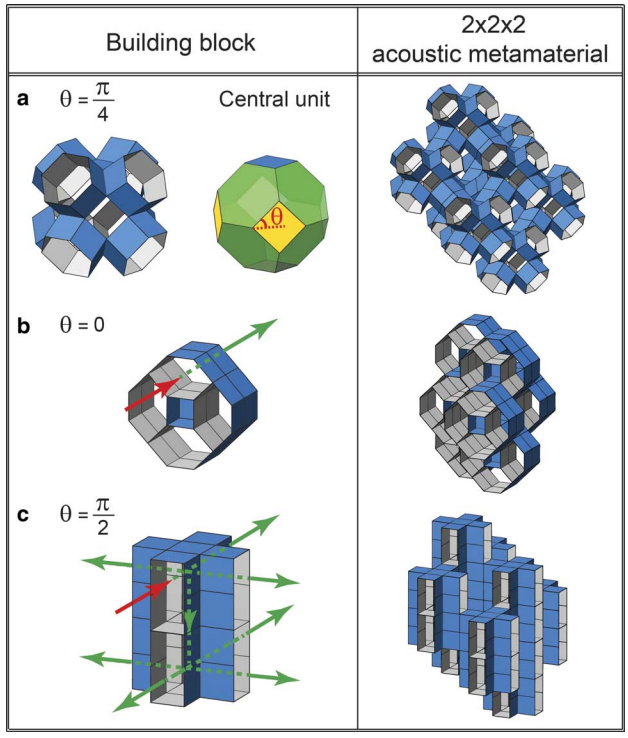

Fig. 6. Reconfigurable acoustic waveguide based on a tessellation of truncated octahedra. Models of the building block and the corresponding reconfigurable acoustic metamaterial deformed into three different configurations: (a) $\theta = \pi/4$, (b) $\theta = 0$, and (c) $\theta = \pi/2$.

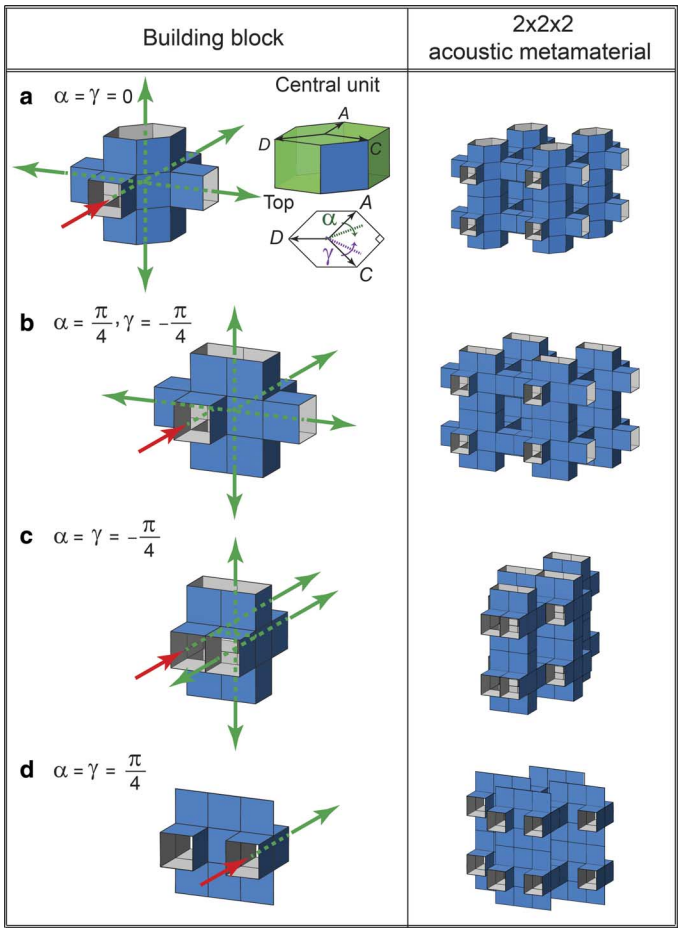

Fig. 7. Reconfigurable acoustic waveguide based on a tessellation of hexagonal prisms. Models of the building block and the corresponding reconfigurable acoustic metamaterial deformed into four different configurations: (a) (α,γ) = (0,0), (b) (α,γ) = (π/4, − π/4), (c) (α,γ) = (−π/4, − π/4), and (d) (α,γ) = (π/4, π/4).

directions (green arrows in Fig. 7A). However, we can transform the metamaterial into a two-dimensional [for (α,γ) = (−π/4, − π/4); Fig. 7C], one-dimensional [for (α,γ) = (π/4, π/4); Fig. 7D], or three-dimensional waveguide with mutually perpendicular channels [for (α,γ) = (π/4, − π/4); Fig. 7B] (see fig. S6 and movie S6).

DISCUSSION

In summary, we propose a new type of reconfigurable acoustic waveguide based on origami principles. Our results indicate that the reconfigurable tubular networks defined by the origami structures can be exploited to achieve very different acoustic responses and wave radiation patterns. The involved acoustic mechanisms are broadband, show a rich behavior in frequency, and can be easily reproduced at different scales (from millimeter- to meter-scale structures).

Note that our strategy to control wave propagation and radiation is based on networks of tubes supporting acoustic waves. These simple systems have not yet been widely studied in this context, as the control of sound wave propagation has been mostly achieved by structuring waveguides with periodic scatterers (*22*–*24*) or resonators (*25*–*27*) in recent years. In most of the reported metamaterials, functionality is locked in place once the metamaterials are fabricated, and tunability is demonstrated by the rotation of the scatterers (*28*–*31*), thermal radiation (*32*), adjustable resonating components (*33*, *34*), and applied mechanical deformation (*35*). However, in all these systems, the tunability is limited to a relatively narrow frequency range. In contrast, the marked reconfiguration of the waveguides proposed here for audible acoustics is broadband and represents a new way of tuning and even switching the propagation of sound. Together, the large number of origami waveguide structures that can be designed, the richness of their deformation modes, and the possibility of using both single-unit cells and complex ensembles leave many opportunities to guide and control the propagation of waves, with possible applications going well beyond the first demonstration of waveguiding and radiation reported here.

MATERIALS AND METHODS

The metamaterial comprising an array of extruded cubes was fabricated from thin PET sheets using an efficient stepwise layering and laser-cutting technique. To fabricate each of the six extruded rhombi that together form a building block (an extruded cube), we used a nearly inextensible polyethylene terephthalate sheet with a thickness (t) of 0.25 mm, covered with a double-sided tape layer (3M VHB Adhesive Transfer Tapes F9460PC) (t = 0.05 mm), and bonded to a second, thinner polyethylene terephthalate layer (t = 0.05 mm). Cutting slits were introduced using a CO_2 laser system (VLS 2.3, Universal Laser Systems); removing the parts from the layered sheet and bonding their ends together could then form the extruded rhombi.

SUPPLEMENTARY MATERIALS

Supplementary material for this article is available at http://advances.sciencemag.org/cgi/content/full/2/11/e1601019/DC1

fig. S1. Propagation of sound waves for (α_1, α_2, α_3) = (π/2, π/2, 0).
fig. S2. Experimental and actual models of the building block (the extruded cube) for (α_1, α_2, α_3) = (π/2, π/2, 0).
fig. S3. Building block and central unit of the metamaterial based on extruded truncated octahedra.
fig. S4. Reconfigurable metamaterial based on a tessellation of truncated octahedra.
fig. S5. Building block and central unit of the extruded truncated octahedron metamaterial.
fig. S6. Reconfigurable metamaterial based on hexagonal prisms.
movie S1. Possible shapes of the extruded cube and the corresponding 4 × 4 × 4 metamaterial.
movie S2. Propagation of sound waves for (α_1, α_2, α_3) = (π/2, π/2, 0).
movie S3. Propagation of sound waves for (α_1, α_2, α_3) = (π/3, 2π/3, π/3).
movie S4. Propagation of sound waves for (α_1, α_2, α_3) = (π/2, π/2, π/2).
movie S5. Possible shapes of the extruded truncated octahedron and the corresponding 4 × 4 × 4 metamaterial.
movie S6. Possible shapes of the extruded hexagonal prism building block and the corresponding 4 × 4 × 4 metamaterial.

REFERENCES AND NOTES

1. A. Selamet, N. S. Dickey, J. M. Novak, The Herschel–Quincke tube: A theoretical, computational, and experimental investigation. *J. Acoust. Soc. Am.* **96**, 3177–3185 (1994).
2. B. Poirier, C. Maury, J.-M. Ville, The use of Herschel–Quincke tubes to improve the efficiency of lined ducts. *Appl. Acoust.* **72**, 78–88 (2011).
3. C. Depollier, J. Kergomard, J. C. Lesueur, Propagation of low frequency acoustic waves in periodic 2D-lattices of tubes. *J. Sound Vib.* **142**, 153–170 (1990).
4. M. Molerón, S. Félix, V. Pagneux, O. Richoux, Sound propagation in periodic urban areas. *J. Appl. Phys.* **111**, 114906 (2012).
5. R. J. Lang, Origami: Complexity increasing. *Eng. Sci.* **52**, 16–23 (1989).
6. J. L. Silverberg, J.-H. Na, A. A. Evans, B. Liu, T. C. Hull, C. D. Santangelo, R. J. Lang, R. C. Hayward, I. Cohen, Origami structures with a critical transition to bistability arising from hidden degrees of freedom. *Nat. Mater.* **14**, 389–393 (2015).

7. H. Yasuda, Z. Chen, J. Yang, Multitransformable leaf-out origami with bistable behavior. *J. Mech. Robot.* **8**, 031013 (2016).
8. B. H. Hanna, J. M. Lund, R. J. Lang, S. P. Magleby, L. L. Howell, Waterbomb base: A symmetric single-vertex bistable origami mechanism. *Smart Mater. Struct.* **23**, 094009 (2014).
9. S. Waitukaitis, R. Menaut, B. G.-g. Chen, M. van Hecke, Origami multistability: From single vertices to metasheets. *Phys. Rev. Lett.* **114**, 055503 (2015).
10. M. Eidini, G. H. Paulino, Unraveling metamaterial properties in zigzag-base folded sheets. *Sci. Adv.* **1**, e1500224 (2015).
11. Z. Y. Wei, Z. V. Guo, L. Dudte, H. Y. Liang, L. Mahadevan, Geometric mechanics of periodic pleated origami. *Phys. Rev. Lett.* **110**, 215501 (2013).
12. H. Yasuda, J. Yang, Reentrant origami-based metamaterials with negative Poisson's ratio and bistability. *Phys. Rev. Lett.* **114**, 185502 (2015).
13. J. L. Silverberg, A. A. Evans, L. McLeod, R. C. Hayward, T. Hull, C. D. Santangelo, I. Cohen, Using origami design principles to fold reprogrammable mechanical metamaterials. *Science* **345**, 647–650 (2014).
14. B. G.-g. Chen, B. Liu, A. A. Evans, J. Paulose, I. Cohen, V. Vitelli, C. D. Santangelo, Topological mechanics of origami and kirigami. *Phys. Rev. Lett.* **116**, 135501 (2016).
15. F. Goldman, Using the snapology technique to teach convex polyhedra, in *Fifth International Meeting of Origami Science, Mathematics, and Education* (CRC Press, 2011), pp. 99–110.
16. H. Strobl, *Special Snapology: A Simple and Cheap Method to Make Convex Polyhedra Models* (2010); http://www.knotology.eu/PPP-Jena2010e/start.html.
17. J. T. B. Overvelde, T. A. de Jong, Y. Shevchenko. S. A. Becerra, G. M. Whitesides, J. C. Weaver, C. Hoberman, K. Bertoldi, A three-dimensional actuated origami-inspired transformable metamaterial with multiple degrees of freedom. *Nat. Commun.* **7**, 10929 (2016).
18. S. Felton, M. Tolley, E. Demaine, D. Rus, R. Wood, A method for building self-folding machines. *Science* **345**, 644–646 (2014).
19. P. M. Morse, K. U. Ingard, *Theoretical Acoustics* (McGraw-Hill, 1987).
20. H. Kuttruff, *Acoustics: An Introduction* (Taylor and Francis, 2014).
21. M. Bruneau, T. Scelo, *Fundamentals of Acoustics* (ISTE, 2006).
22. C. E. Bradley, Time harmonic acoustic bloch wave propagation in periodic waveguides. Part I. Theory. *J. Acoust. Soc. Am.* **96**, 1844–1853 (1994).
23. M. S. Kushwaha, A. Akjouj, B. Djafari-Rouhani, L. Dobrzynski, J. O. Vasseur, Acoustic spectral gaps and discrete transmission in slender tubes. *Solid State Comm.* **106**, 659–663 (1998).
24. J. N. Munday, C. B. Bennett, W. M. Robertson, Band gaps and defect modes in periodically structured waveguides. *J. Acoust. Soc. Am.* **112**, 1353–1358 (2002).
25. N. Sugimoto, M. Masuda, J. Ohno, D. Motoi, Experimental demonstration of generation and propagation of acoustic solitary waves in an air-filled tube. *Phys. Rev. Lett.* **83**, 4053–4057 (1999).
26. O. Richoux, V. Tournat, T. Le Van Suu, Acoustic wave dispersion in a one-dimensional lattice of nonlinear resonant scatterers. *Phys. Rev. E* **75**, 026615 (2007).
27. J.-P. Groby, W. Huang, A. Lardeau, Y. Aurégan, The use of slow waves to design simple sound absorbing materials. *J. Appl. Phys.* **117**, 124903 (2015).
28. C. Goffaux, J. P. Vigneron, Theoretical study of a tunable phononic band gap system. *Phys. Rev. B* **64**, 075118 (2001).
29. V. Romero-García, C. Lagarrigue, J.-P. Groby, O. Richoux, V. Tournat, Tunable acoustic waveguides in periodic arrays made of rigid square-rod scatterers: Theory and experimental realization. *J. Phys. D Appl. Phys.* **46**, 305108 (2013).
30. F. Wu, Z. Liu, Y. Liu, Acoustic band gaps created by rotating square rods in a two-dimensional lattice. *Phys. Rev. E* **66**, 046628 (2002).
31. Sz.-C. S. Lin, T. J. Huang, Tunable phononic crystals with anisotropic inclusions. *Phys. Rev. B* **83**, 174303 (2011).
32. E. Walker, D. Reyes, M. M. Rojas, A. Krokhin, Z. Wang, A. Neogi, Tunable ultrasonic phononic crystal controlled by infrared radiation. *Appl. Phys. Lett.* **105**, 143503 (2014).
33. F. Casadei, T. Delpero, A. Bergamini, P. Ermanni, M. Ruzzene, Piezoelectric resonator arrays for tunable acoustic waveguides and metamaterials. *J. Appl. Phys.* **112**, 064902 (2012).
34. G. Theocharis, O. Richoux, V. Romero-García, A. Merkel, V. Tournat, Limits of slow sound propagation and transparency in lossy, locally resonant periodic structures. *New J. Phys.* **16**, 093017 (2014).
35. S. Babaee, N. Viard, P. Wang, N. X. Fang, K. Bertoldi, Harnessing deformation to switch on and off the propagation of sound. *Adv. Mat.* **28**, 1631–1635 (2016).

Acknowledgments

Funding: This work was supported by the Harvard Materials Research and Engineering Center through grant DMR-1420570 and by the NSF through grant CMMI-1149456 (CAREER). E.R.C. acknowledges NSF MSPRF grant DMS-1204686. V.T. acknowledges grants from Direction Générale de l'Armement and Centre National de la Recherche Scientifique. **Author contributions:** S.B., J.T.B.O., V.T., and K.B. provided research motivation, designed the analyses, evaluated and interpreted the results, and wrote the article. S.B. and E.R.C. developed the analytical model for possible configurations of the metamaterial models. S.B. and K.B. performed the numerical analysis. J.T.B.O. fabricated the sample. S.B. and V.T. carried out the experimental measurements. **Competing interests**: All authors declare that they have no competing interests. **Data and materials availability**: All data needed to evaluate the conclusions in the paper are present in the paper and/or the Supplementary Materials. Additional data related to this paper may be requested from the authors.

Submitted 6 May 2016
Accepted 21 October 2016
Published 23 November 2016
10.1126/sciadv.1601019

Citation: S. Babaee, J. T. B. Overvelde, E. R. Chen, V. Tournat, K. Bertoldi, Reconfigurable origami-inspired acoustic waveguides. *Sci. Adv.* **2**, e1601019 (2016).

ScienceAdvances
AAAS

Reconfigurable origami-inspired acoustic waveguides
Sahab Babaee, Johannes T. B. Overvelde, Elizabeth R. Chen, Vincent Tournat and Katia Bertoldi (November 23, 2016)
Sci Adv 2016, 2:.
doi: 10.1126/sciadv.1601019